



## Letter

Plasma electrolytic oxidation preparation and characterization of SnO<sub>2</sub> filmJ. He<sup>a</sup>, Q.Z. Cai<sup>a,\*</sup>, F. Xiao<sup>b</sup>, X.W. Li<sup>a</sup>, W. Sun<sup>a</sup>, X. Zhao<sup>a</sup><sup>a</sup> State Key Lab of Material Processing and Dies & Mould Technology, Huazhong University of Science and Technology, Wuhan 430074, China<sup>b</sup> College of Wenhua, Huazhong University of Science and Technology, Wuhan 430074, China

## ARTICLE INFO

## Article history:

Received 9 December 2009

Received in revised form

19 September 2010

Accepted 21 September 2010

Available online 1 October 2010

## Keywords:

SnO<sub>2</sub>

Plasma electrolytic oxidation

Stannate electrolyte

Photocatalysis

## ABSTRACT

SnO<sub>2</sub> film is firstly prepared by plasma electrolytic oxidation technology in sodium stannate solution. The structure and photocatalytic property of the film are characterized by SEM, XRD and UV-Vis spectrophotometer. Rough and porous netlike film formed on the substrate. The XRD result showed the oxide was pure SnO<sub>2</sub>. The absorption edge of the film was determined as 420 nm. Photocatalytic degradation of rhodamine indicated SnO<sub>2</sub> film was an effective photocatalyst.

© 2010 Elsevier B.V. All rights reserved.

## 1. Introduction

SnO<sub>2</sub> is used to photocatalytic decontamination treatment of polluted water and air purification due to its excellent chemical stability and unique catalytic property [1,2]. To date, most of the ongoing research on SnO<sub>2</sub> photocatalysis focuses on the use of nanocrystalline powder. However, the use of SnO<sub>2</sub> powder in photocatalysis is difficult due to that power is hard to separate, recycle and reuse. So, SnO<sub>2</sub> must be immobilized in films to be useful in any practical photocatalytic application.

Plasma electrolytic oxidation (PEO) has widely used to prepare oxide film on the Al, Mg and Ti [3,4]. The distinct properties of oxide film formed via PEO include high porosity, remarkable thickness and good adhesion to the metal substrates. Furthermore, the composition and structure of PEO film can be changed by adding different electrolyte ionic compositions. Our previous research [5] reveals that WO<sub>3</sub> can be generated when titanium is plasma electrolytic oxidized in electrolyte containing WO<sub>4</sub><sup>2-</sup>. On this basis, we attempt to synthesis SnO<sub>2</sub> film by PEO technology in solution containing SnO<sub>3</sub><sup>2-</sup>.

In this study, SnO<sub>2</sub> film is prepared by PEO in sodium stannate solution. The structure and photocatalytic property of film are investigated.

## 2. Experimental

The setup of plasma electrolytic oxidation consisted of ambipolar impulsing power source, electrolytic cell, mixing system, cooling system and exhaust system. The sketch map of setup is presented in Fig. 1.

A pure titanium (99.9%) sheet with dimensions 20 mm × 20 mm × 2 mm was selected as base material, polished with emery papers (#400–#1200 grit) and degreased using acetone followed by rinsing with distilled water. The electrolyte consisted of 10.7 g/L Na<sub>2</sub>SnO<sub>3</sub>, 2 g/L NaOH and 2 g/L NaF. A pure titanium sheet was used as an anode and a stainless steel plate was used as cathode. The positive voltage, negative voltage, frequency, duty cycle and treatment period were 300 V, –30 V, 700 Hz, 0.3 and 5 min, respectively. The temperature of electrolyte was kept at the range of 25–40 °C through circulating water cooling system during the complete PEO process. The prepared SnO<sub>2</sub> film was rinsed in distilled water, dried in hot air and then kept in a drying chamber. In order to compare the photocatalytic activity of SnO<sub>2</sub> film with TiO<sub>2</sub> film, we also prepared the TiO<sub>2</sub> film. The electrolyte for preparing TiO<sub>2</sub> film consisted of 10.7 g/L Na<sub>3</sub>PO<sub>4</sub>, 2 g/L NaOH and 2 g/L NaF, and the other parameters and processes were the same with SnO<sub>2</sub> film.

The morphologies of film were characterized by Quanta 200 scanning electron microscopy. The crystal structure was determined by X-ray diffractometer using Cu Kα. The UV-Vis absorption spectra of film were recorded on a Shimadzu UV-2550 spectrophotometer with an integrating sphere.

Photocatalytic activity of film was determined by photodegradation of rhodamine in aqueous solution. The film was pre-saturated in 10 ml of 10 mg/L rhodamine solution at dark for 30 min to reach adsorption/desorption equilibrium. A 365 nm ultraviolet germicidal lamp with 40 W was used as light source. The solution was constantly supplied with air during the reaction.

For the purpose of determining photocatalytic activity of film, the absorbance of rhodamine solution at 550 nm was tested by a Shimadzu UV-2550 spectrophotometer. Because the absorbance of dilute solution is linear with its concentration according to Lambert-Beer Law [6], degradation percentage of rhodamine  $\eta$  can be calculated according to the formula (1)

$$\eta = \frac{A_0 - A}{A_0} \times 100\% \quad (1)$$

\* Corresponding author. Fax: +86 27 87541922.

E-mail address: [caiqizhou@mail.hust.edu.cn](mailto:caiqizhou@mail.hust.edu.cn) (Q.Z. Cai).

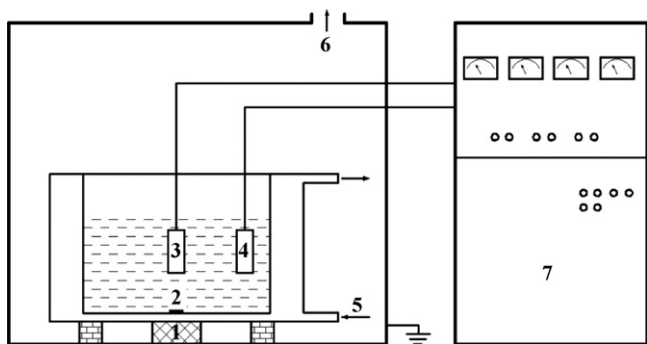


**Fig. 1.** Sketch map of plasma electrolytic oxidation setup: 1 magnetic stirrer; 2 rotor; 3 titanium sheet; 4 counter electrode; 5 circulating cooling system; 6 exhaust system; 7 power source.

where  $A_0$  is the initial absorbance of rhodamine solution,  $A$  is the absorbance of rhodamine solution when photocatalytic reaction is finished.

### 3. Results and discussion

#### 3.1. Surface and cross-sectional morphologies of film

The SEM micrographs of  $\text{SnO}_2$  film are presented in Fig. 2. Rough and porous netlike film forms on the titanium substrate. The formation of such highly branched structures is caused by gas generation during the film process. All the pores are well separated and homogeneously distribute over the surface. Cross-sectional views of  $\text{SnO}_2$  film reveal a dense morphology. The thickness of film is estimated to be  $80\ \mu\text{m}$ . There is no obvious discontinuity between the film

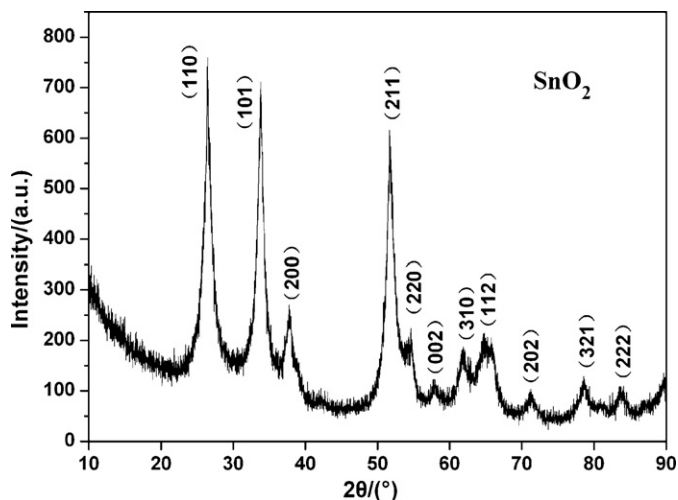


**Fig. 3.** XRD patterns of  $\text{SnO}_2$  film.

and the underlying substrate. It appears that the  $\text{SnO}_2$  film is well adhered to the substrate.

#### 3.2. XRD analysis of film

Fig. 3 shows XRD patterns of  $\text{SnO}_2$  film. All peaks are assigned to  $\text{SnO}_2$ . The peaks of  $\text{SnO}_2$  are wide, which means the grain of  $\text{SnO}_2$  is rather small. The grain size of  $\text{SnO}_2$  is calculated by Scherrer formula and determined as  $60\ \text{nm}$ . The experimental diffraction peaks and that of JCPDS data are tabulated in Table 1 [7].

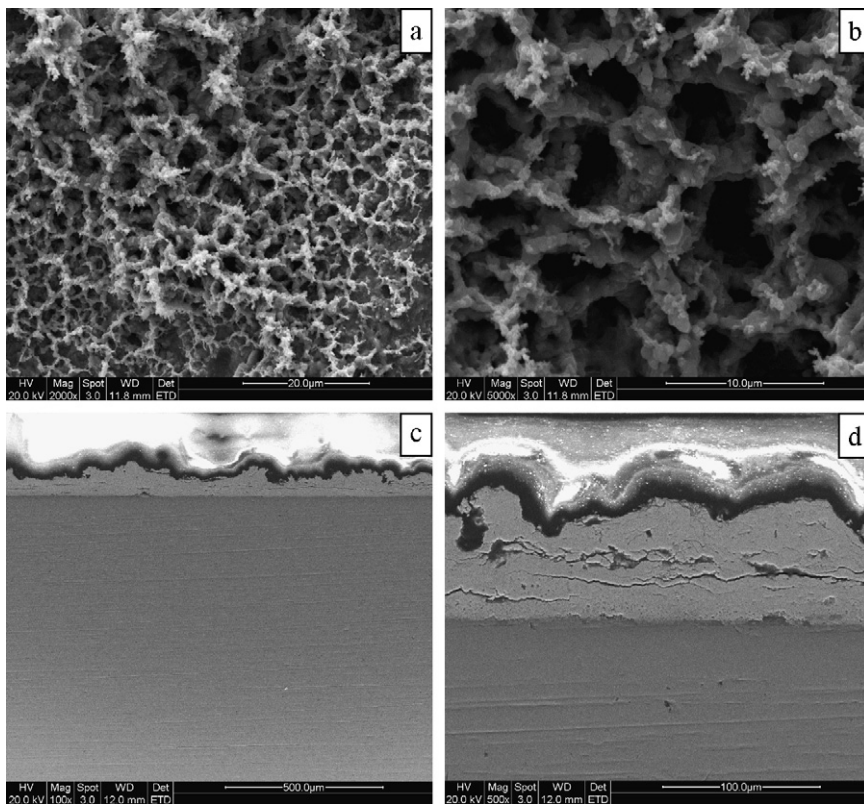


**Fig. 2.** Morphologies of  $\text{SnO}_2$  film: (a and b) surface; (c and d) cross-section.

**Table 1**  
Experimental and JCPDS data diffraction peak positions of SnO<sub>2</sub> phase.

(hkl)	Experimental (2θ)	Literature (2θ)
(1 1 0)	26.462	26.589
(1 0 1)	33.823	33.877
(2 0 0)	37.804	37.956
(2 1 1)	51.656	51.777
(2 2 0)	54.634	54.762
(0 0 2)	57.876	57.828
(3 1 0)	61.861	61.887
(1 1 2)	64.772	64.741
(2 0 2)	71.230	71.279
(3 2 1)	78.591	78.714
(2 2 2)	83.676	83.717

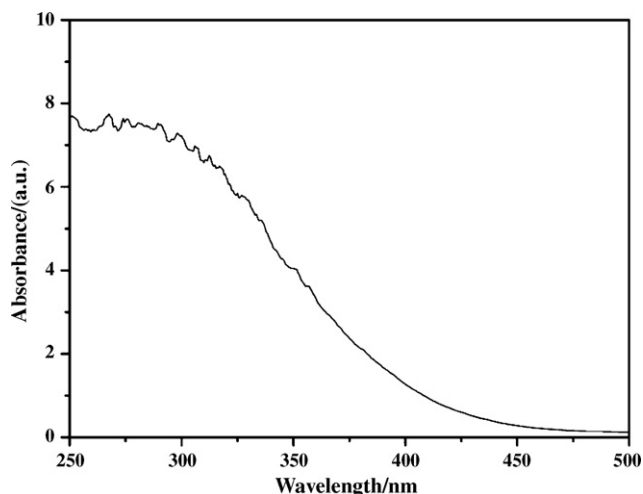


Fig. 4. UV-Vis absorption spectrum of SnO<sub>2</sub> film.

The forming reason of SnO<sub>2</sub> film can be interpreted as follows. SnO<sub>3</sub><sup>2-</sup> could be uniformly absorbed at the surface of anode under electric field, and decomposed into SnO<sub>2</sub> under the elevated temperature generated by micro-plasma discharge. As-deposited SnO<sub>2</sub> forms film at the surface of anode.

### 3.3. UV-Vis diffuse reflectance spectra of film

Fig. 4 shows the UV-Vis diffuse reflectance spectra of SnO<sub>2</sub> film. The oxide film reveals excellent absorption of UV light. The absorption edge of SnO<sub>2</sub> film occurs at 420 nm, and the band gap  $E_g$  is calculated according to the formula (2)

$$E_g = \frac{hc}{\lambda} = \frac{1243.1}{\lambda} \quad (2)$$

where  $E_g$  is the band gap (eV) of the film,  $h$  is the Planck's constant ( $4.135667 \times 10^{-15}$  eV s),  $c$  is the velocity of light ( $3 \times 10^8$  m/s),  $\lambda$  is the cut-off wavelength of the spectra (nm), and the unit of 1243.1 is eV nm. The band gap energy of SnO<sub>2</sub> film is calculated to be 2.95 eV, which is considerably less than the well-known SnO<sub>2</sub> band gap of 3.5–3.6 eV. The reason of this discrepancy is not very clear and being investigated now.

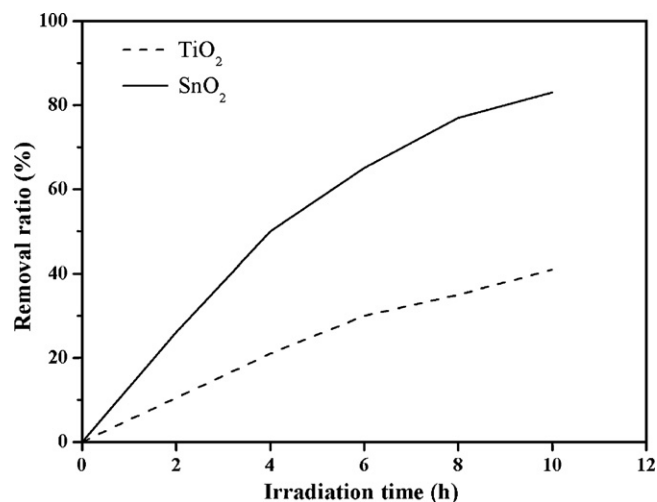


Fig. 5. Removal ratio of rhodamine as a function of irradiation time.

### 3.4. Photo-degradation of rhodamine

No detectable degradation of rhodamine occurs without SnO<sub>2</sub> film and TiO<sub>2</sub> film. The removal ratio of rhodamine is presented in Fig. 5. The result indicates that about 83% of rhodamine is degraded by SnO<sub>2</sub> film within 10 h of UV irradiation whereas about 41% of rhodamine is degraded by TiO<sub>2</sub> film within 10 h of UV irradiation, so photocatalytic activity of SnO<sub>2</sub> film is higher than that of TiO<sub>2</sub> film.

The porous surface structure should be responsible for providing more surface sites, in which holes could react with adsorbed molecules. Excellent absorption ensures many photons absorbed to generate holes, which has very strong oxidizing power due to the valence band of SnO<sub>2</sub> lying more positive than TiO<sub>2</sub>. Both contribute to photocatalytic degradation of rhodamine.

## 4. Conclusions

SnO<sub>2</sub> film was successfully produced by the plasma electrolytic oxidation technique in stannate electrolyte. SnO<sub>2</sub> film presented porous netlike surface and high absorption in UV region, which were responsible for its high photocatalytic activity. Future works will focus on the further improvement of photocatalytic activity of SnO<sub>2</sub> film by adjusting process parameters, such as power voltage, reaction time, electrolyte composition, etc.

## References

- [1] Z.H. Wen, G. Wang, W. Lu, Q. Wang, Q. Zhang, J.H. Li, *Crystal Growth Des.* 7 (9) (2007) 1722–1725.
- [2] Y. Zhang, A. Kolmakov, Y. Lilach, M. Moskovits, *J. Phys. Chem. B* 109 (5) (2005) 1923–1929.
- [3] W. Xue, Z. Deng, R. Chen, T. Zhang, *Thin Solid Films* 372 (2000) 114.
- [4] G. Sundarajan, L.R. Krishna, *Surf. Coat. Technol.* 167 (2003) 269.
- [5] J. He, Q.Z. Cai, Y.G. Ji, H.H. Luo, D.J. Li, B. Yu, *J. Alloys Compd.* 482 (2009) 476.
- [6] K. Danzer, *Analytical Chemistry*, Springer, Berlin/Heidelberg, 2007.
- [7] A.A. Bolzan, et al., *Acta Crystallogr. B: Struct. Sci.* 53 (1997) 373.